Macromolecular Research

Article

DOI 10.1007/s13233-021-9023-6

www.springer.com/13233 pISSN 1598-5032 eISSN 2092-7673

Conductive and Stable Crosslinked Anion Exchange Membranes Based on Poly(arylene ether sulfone)

Joseph Jang[†,1]
Min-Kyoon Ahn[†,1]
Su-Bin Lee[1]
Cheong-Min Min[1]
Beom-Goo Kang[*,2]
Jae-Suk Lee[*,1]

[1] School of Materials Science and Engineering, Gwangju Institute of Science and Technology (GIST), Gwangju 61005, Korea
[2] Department of Chemical Engineering, Soongsil University, Seoul 06978, Korea

Received October 28, 2020 / Revised January 20, 2021 / Accepted January 20, 2021

Abstract: Highly conductive and stable anion exchange membranes (AEMs) are important components of high-performance anion exchange membrane fuel cells (AEMFCs). Here, we report the use of crosslinked poly(arylene ether sulfone) (PAES) AEMs containing quaternary ammonium (QA) and triazolium cations. The crosslinked PAES-triazole-hydroxide membrane (cPAES-TA-OH) had a higher ion exchange capacity (IEC) than that of the non-crosslinked membrane (PAES-TA-OH) owing to the presence of triazolium cations. The IEC values of cPAES-TA-OH and PAES-TA-OH were 1.75 and 1.31 meq/g, respectively. The IEC value affects the water uptake and swelling ratio of a membrane. The water uptake and swelling ratio of cPAES-TA-OH were higher than those of PAES-TA-OH at 30 °C and 80 °C. In addition, hydroxide conductivity and membrane stability were enhanced by crosslinking; the hydroxide conductivity of cPAES-TA-OH was 92.1 mS/cm at 80 °C under 95% RH (in contrast to 86.2 mS/cm for PAES-TA-OH), and its conductivity retention was 67% after treating with 1 M NaOH at 80 °C for 24 h (in contrast to 51% for PAES-TA-OH).

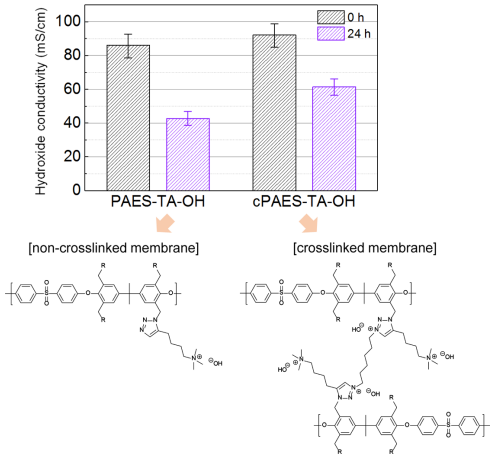

Keywords: AEMFCs, crosslinking, triazolium, quaternary ammonium, alkaline stability.

1. Introduction

Recently, anion exchange membrane fuel cells (AEMFCs) have been considered as potential power-generating energy devices owing to their favorable electrochemical kinetics and high energy conversion. In addition, non-precious metals are used as catalysts.[1-5] For these cells to exhibit high performance, anion exchange membranes (AEMs) should be highly conductive and dimensionally stable. In addition, the alkaline stability of AEMs is important for the long-term durability of AEMFCs as these cells are operated under highly basic conditions.[2,3]

Crosslinking is a promising approach to improve the fuel cell performance of AEMs. Wang *et al.* reported azide-assisted self-crosslinked AEMs based on polystyrene and poly(*p*-phenylene oxide). The crosslinking was effective in terms of alkaline stability; the bicarbonate conductivity of the crosslinked membranes remained at ~90% of their initial values after the test of 400 h even at 10 M of NaOH at 80 °C.[6] Lee *et al.* reported the end-group crosslinking of AEMs. The crosslinking was simply formed by thermal heating, and the degree of crosslinking was dependent on the heating time. The crosslinking density influenced the membrane morphology, hydroxide conductivity, and fuel cell performance.[7]

Cations are key materials in AEMs because cation groups and hydroxide ions bind to each other; hydroxide ions facilitate ion transport in the water electrolyte medium through the hydrogen bonding network,[8] and the structure of cations is effective for alkaline stability.[9] Quaternary ammonium (QA) cations and imidazolium cations have been most often used as cation groups in AEMs.[1-5] Triazole moiety is also a promising functional group for AEMs because it can facilitate the formation of a continuous hydrogen bonding network.[6,10,11] Moreover, triazole groups can be easily converted into triazolium cations. However, very few studies on AEMs containing triazolium groups have been conducted so far. Guiver *et al.* reported the potential use of triazolium-based AEMs.[12] The membranes functionalized with triazolium cations showed comparable hydroxide conductivity and higher alkaline stability compared to those obtained using imidazolium cation-functionalized membranes.

In this study, we prepared novel crosslinked poly(arylene ether sulfone) (PAES) AEMs. The QA cations and triazole groups were introduced to PAES by the copper(I)-catalyzed alkyne-azide cycloaddition (CuAAC) "click reaction", and the triazole moieties were subsequently converted into triazolium cations by *in-situ* casting and crosslinking. The influence of crosslinking on membrane performance was investigated by comparing the cross-

Acknowledgments: This work was supported by the National Strategic Project - Fine Particle of the National Research Foundation of Korea (NRF) funded by the Ministry of Science and ICT (MSIT), Ministry of Environment (ME), and Ministry of Health and Welfare (MOHW) (2017M3D8A1091937).

***Corresponding Authors:** Beom-Goo Kang (bkang@ssu.ac.kr), Jae-Suk Lee (jslee@gist.ac.kr)
[†]These authors equally contributed to this work.

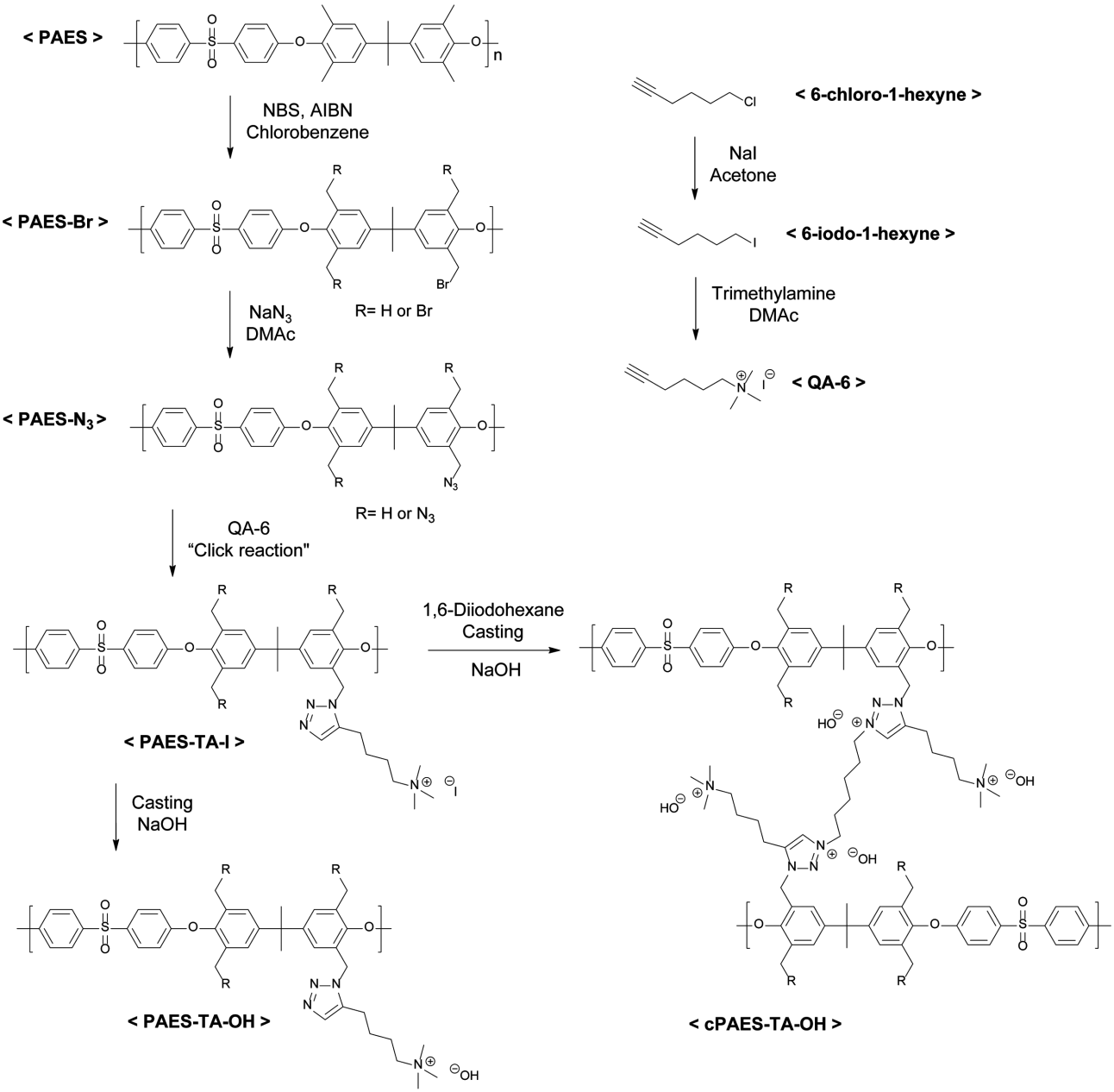

Scheme 1. Preparation of PAES-TA-OH and cPAES-TA-OH membranes.

linked PAES-triazole-hydroxide membrane (cPAES-TA-OH) with a non-crosslinked membrane (PAES-TA-OH). It should be worth noting that the crosslinking led to the improved AEM properties and offset the trade-off between hydroxide conductivity and stability of crosslinked membranes. The synthetic details, ion exchange capacity (IEC), water uptake, swelling ratio, hydroxide conductivity, and alkaline stability results are discussed.

2. Experimental

2.1. Materials

N-Bromosuccinimde (NBS), 2,2′-azobis(2-methylpropionitrile) (AIBN), copper(I) bromide (CuBr), *N,N,N′,N″,N*‴-pentamethyldiethylene triamine (PMDETA), sodium iodide (NaI), potassium carbonate (K_2CO_3), and 4,4′-isopropylidene bis(2,6-dimethylphenol) were purchased from Sigma-Aldrich. Chlorobenzene, sodium azide (NaN_3), 1,6-diiodohexane (DIH), trimethylamine (TMA), and bis(4-fluorophenyl) sulfone were purchased from Tokyo Chemical Industry. 6-Chloro-1-hexyne, *N,N*-dimethylacetamide (DMAc), *N,N*-dimethylformamide (DMF), and *N*-methyl-2-pyrrolidone (NMP) were supplied by Alfa Aesar and used as received.

2.2. Measurements

Proton nuclear magnetic resonance (^{1}H NMR) spectroscopy measurements were recorded using a JEOL JNM-LA 400 WB FT-NMR spectrometer, with DMSO-d_6 as a solvent. Fourier transform infrared (FT-IR) spectroscopy measurements were recorded using

an FT-IR spectrometer (FT/IR 460 Plus, Jasco, Japan) with a MiracleTM accessory (PIKE Tech. Inc., USA). The thermal stability of the membranes was determined using a 2100 series TA instrument. Thermal degradation was determined by thermogravimetric analysis (TGA) in the temperature range from 30 °C to 800 °C at a heating rate of 10 °C/min in nitrogen atmosphere.

2.3. Synthesis of QA-6

6-Iodo-1-hexyne was obtained by halide exchange with NaI as follows: 6-chloro-1-hexyne, NaI, and acetone were placed in a one-neck flask. The solution was refluxed at 60 °C for 12 h. After removing acetone, the yellow compounds were extracted with chloroform/water and dried with Na_2SO_4. Then, QA-6 was obtained by S_N2 reaction of 6-iodo-1-hexyne and excess TMA at 40 °C for 12 h in DMAc. ^{1}H NMR (400 MHz, DMSO-d_6): δ = 1.37-1.48 (C≡C-C**H**$_2$), 1.66-1.79 (C≡C-CH$_2$-C**H**$_2$), 2.16-2.26 (C**H**$_2$-CH$_2$-N), 2.81-2.85 (**H**C≡C), 2.95-3.07 (N(C**H**$_3$)$_3$), and 3.23-3.33 (C**H**$_2$-N).

2.4. Synthesis of PAES

PAES copolymers were synthesized by aromatic condensation polymerization as described in our previous study.[13] A mixture of 4,4′-Isopropylidene bis(2,6-dimethylphenol), K_2CO_3, DMAc, and benzene was stirred in nitrogen atmosphere. After removing benzene and water, bis(4-fluorophenyl) sulfone in DMAc was added into the flask, and the solution was kept stirred at 160 °C for 20 h. Then, the reaction solution was cooled and poured into ethanol. The precipitated polymer was collected and washed with ethanol several times and then dried in a vacuum oven at 60 °C.

2.5. Synthesis of PAES-Br

Brominated PAES (PAES-Br) was synthesized by benzylic radical substitution reaction, as described in our previous study.[13] PAES, NBS, and AIBN were dissolved in chlorobenzene. The reaction solution was kept at 135 °C for 6 h with vigorous stirring under nitrogen atmosphere. Then, the solution was cooled and precipitated into ethanol. The precipitated polymer was collected and washed with ethanol several times and then dried in a vacuum oven at 60 °C.

2.6. Synthesis of PAES-N_3

Azido PAES (PAES-N_3) was synthesized by S_N2 reaction as described in our previous study.[13] A mixture of PAES-Br, NaN_3, and DMAc was stirred at 60 °C overnight under nitrogen atmosphere. Then, the reaction solution was cooled and precipitated into ethanol. The precipitated polymer was collected and washed with ethanol and deionized (DI) water several times and then dried in a vacuum oven at 60 °C.

2.7. Synthesis of PAES-TA-I

QA cations were introduced to PAES-N_3 by a click reaction with QA-6. A mixture of PAES-N_3, QA-6, CuBr, PMDETA, and DMF was stirred until all reagents completely dissolved. The flask was degassed by three freeze-pump-thaw cycles to remove the oxygen in the flask. The reaction solution was heated at 60 °C and stirred overnight under nitrogen atmosphere. Then, the reaction solution was cooled and precipitated into ethanol. The precipitated polymer was collected and washed several times with ethanol and DI water. The resulting polymer was dried in a vacuum oven at 60 °C. ^{1}H NMR (400 MHz, DMSO-d_6): δ = 1.38-1.53 (C=C-CH$_2$-C**H**$_2$), 1.53-1.72 (C**H**$_3$-C-C**H**$_3$, C**H**$_2$-CH$_2$-N), 1.86-2.00 (phenyl-C**H**$_3$), 2.66-2.73 (triazole-C**H**$_2$), 2.82-2.89 (CH$_2$-C**H**$_2$-N), 2.95-3.10 (N(C**H**$_3$)$_3$), 5.23-5.41 (triazole-C**H**$_2$-phenyl), 6.74-7.74 (phenyl), and 7.75-7.94 (triazole).

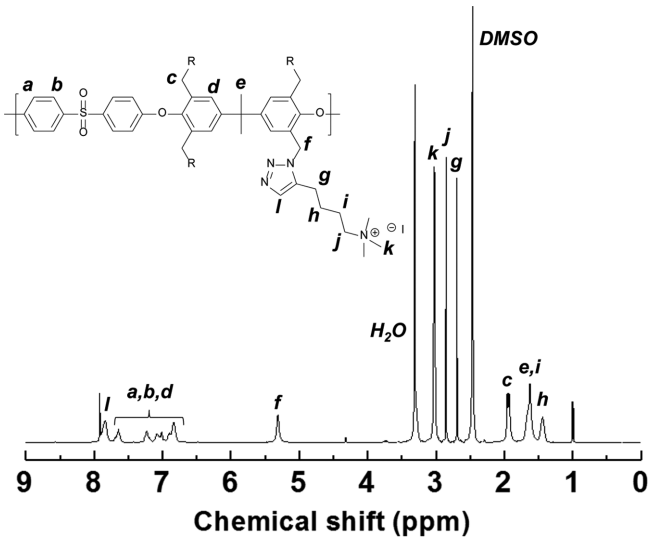

Figure 1. ^{1}H NMR spectrum of PAES-TA-I.

2.8. Membrane preparation

PAES-TA-I was dissolved in NMP (10 w/v%) and stirred vigorously until the solution became homogeneous. Then, DIH (0.25 equivalent to the triazole of PAES-TA-I) was added to the flask. The solution was filtered and the filtrate was poured onto a clean glass hot plate. The temperature was kept at 80 °C over 12 h. The crosslinked membrane was immersed in DI water to be peeled off from the glass plate. The cPAES-TA-OH membrane was obtained by exchanging iodide ions to hydroxide ions in 0.5 M NaOH at room temperature for 24 h. The non-crosslinked membrane, PAES-TA-OH, was prepared by a similar procedure.

2.9. IEC measurements

The IECs were measured using a classical titration method. The dried membranes were immersed in 0.05 M HCl for 24 h. After removing the membranes, the remaining liquid was titrated against 0.05 M NaOH using phenolphthalein as an indicator. The IECs were expressed and calculated using the following equation:

$$\text{IEC (meq/g)} = \frac{\left(\text{Consumed HCl} \times \text{Molarity HCl}\right) - \left(\text{Consumed NaOH} \times \text{Molarity NaOH}\right)}{\text{Weight of dried membrane}} \quad (1)$$

2.10. Water uptake and swelling ratio measurements

The membranes were prepared by vacuum drying at 80 °C. The dried membranes were then immersed in DI water at 30 °C and 80 °C and periodically weighed on an analytical balance until constant water uptake weights were obtained. The water uptake and swelling ratio of the membranes were calculated using the following equations:

$$\text{Water uptake (\%)} = \frac{W_{wet} - W_{dry}}{W_{dry}} \times 100 \quad (2)$$

where W_{wet} is the weight of the wet membranes and W_{dry} is the weight of the dried membranes;

$$\text{Swelling ratio (\%)} = \frac{l_{wet} - l_{dry}}{l_{dry}} \times 100 \quad (3)$$

where l_{wet} is the length of the wet membranes and l_{dry} is the length of the dried membranes.

2.11. Hydroxide conductivity measurements

Hydroxide conductivity was measured using a four-point probe method. The membranes were put inside of a homemade in-plain conductivity cell and kept in a thermos-hygrostat (SH-241, ESPEC). All measurements were recorded at 30 °C and 80 °C in 95% relative humidity (RH) under air. The impedance was measured using an electrochemical impedance analyzer (Solatron 1280Z) over a frequency range from 1 Hz to 20 kHz. Using a Bode plot, the frequency region over which the impedance had a constant value was measured, and the resistance was obtained from a Nyquist plot. The hydroxide conductivity was calculated as follows:

$$\sigma = L/RS \quad (4)$$

where σ (S/cm or $W^{-1}cm^{-1}$) is the hydroxide conductivity, L (cm) is the distance between the two electrodes, R (Ω) is the resistance of the membrane, and S (cm^2) is the surface area of the membrane. The impedance of each sample was measured at least five times to ensure reproducibility of the data.

3. Results and discussion

3.1. Preparation and characterization of membranes

The preparation of PAES-TA-OH and cPAES-TA-OH membranes is shown in Scheme 1. PAES-N_3 with 25% degree of azidation was synthesized according to the procedure described in our previous work.[13] Triazole groups and QA cations were then introduced by the click reaction of QA-6 and PAES-N_3. As shown in Figure 1, the chemical structure of PAES-TA-I was confirmed by ^{1}H NMR. The characteristic proton peak observed at 7.75-7.94 ppm verified the formation of triazole by the alkyne-azide cycloaddition click reaction. FT-IR characterization of PAES-N_3 and PAES-TA-I strongly supported the successful preparation of PAES-TA-I (Figure 2). While the characteristic peak at 2100 cm^{-1} corresponding to the azide groups completely disappeared after the click reaction, the spectrum of PAES-TA-I showed a broad peak at 3400 cm^{-1} corresponding to the O-H stretching vibration.[14,15] The

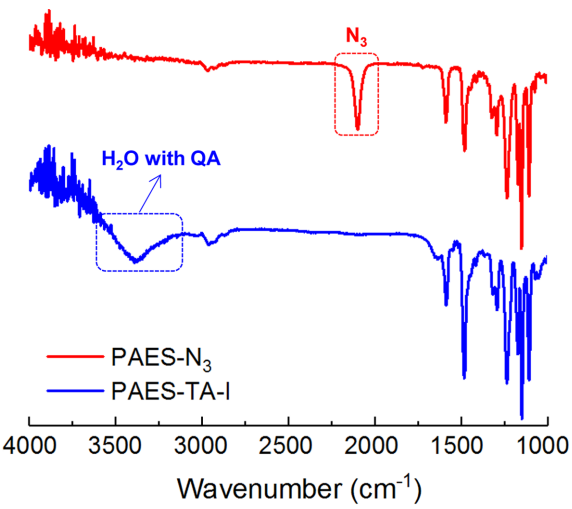

Figure 2. FT-IR spectra of PAES-N_3 and PAES-TA-I.

new peak at 3400 cm^{-1} indicates that the introduction of QA cations help water molecules to get absorbed into PAES-TA-I.

The cPAES-TA-OH membrane was then prepared by *in-situ* casting and thermal crosslinking, followed by ion exchange using NaOH. 1,6-Diiodohexane (DIH) was chosen as the crosslinker since DIH gave the enough toughness and flexibility of the crosslinked membrane. When 1,4-diiodobutane (DIB) and 1,8-diiodooctane (DIO) were used as the crosslinkers, DIB caused brittleness of the crosslinked membrane due to the short carbon length, whereas thermal crosslinking with DIO did not proceed well because of the long carbon length, leading to a weak membrane. This result indicates the importance of the length of crosslinking to fabricate physically stable membranes.[15,16] The non-crosslinked PAES-TA-OH membrane was similarly prepared with cPAES-TA-OH, except for the crosslinking step. Figure 3 shows that the crosslinking reaction of PAES-TA-I and DIH was thermally activated, and covalent bonding was formed under the fabrication conditions of the cPAES-TA-OH membrane. The crosslinked membrane was homogeneous, transparent, and physically stable as other membranes produced by thermal crosslinking.[4,7,17-19] To confirm the successful crosslinking of cPAES-TA-OH, a solubility test of the membranes was carried out. The PAES-TA-OH membrane was dissolved after immersion in NMP at 80 °C for 12 h,

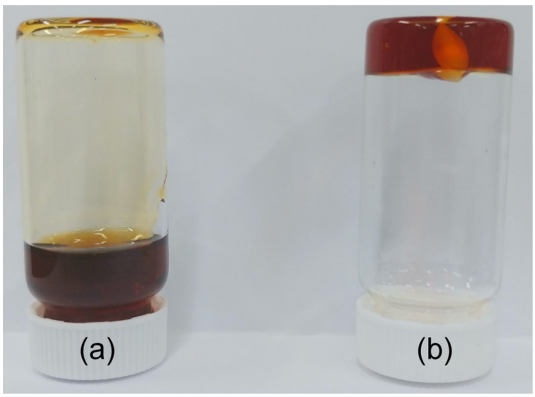

Figure 3. PAES-TA-I and DIH solution in NMP (a) before and (b) after heating at 80 °C for 12 h.

Table 1. Gel fraction, degradation temperature, and IEC values of membranes

Membranes	Gel fraction (%)	$T_{d5\%}$ (°C)	IEC (meq/g)	
			Calc.	Titr.
PAES-TA-OH	0	189	1.43	1.31
cPAES-TA-OH	> 75	186	2.13	1.75

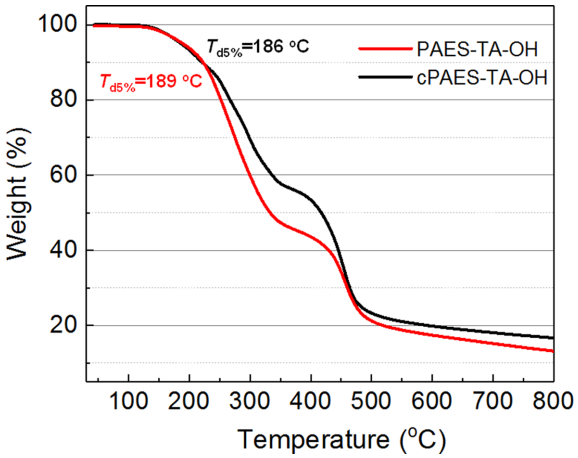

Figure 4. TGA thermograms of PAES-TA-OH and cPAES-TA-OH.

but the cPAES-TA-OH membrane showed more than 75% gel fraction under the same conditions (Table 1).

3.2. Thermal stability

Thermal stability of the membranes was investigated using TGA (Figure 4). The membranes showed similar two-step degradation curves. The first degradation from 150 °C to 350 °C is attributed to the degradation of triazoles, triazolium cations, and QA cations.[12,20] Although the 5% weight degradation temperatures ($T_{d5\%}$) of the two membranes were similar, the first degradation behaviors were different. This may be due to the crosslinked structure of the cPAES-TA-OH.[21,22] The compact crosslinked structure would have slowed the heat conduction into the inside of the membrane. The second weight loss between 350 °C and 500 °C was associated with the degradation of the polymer main chains.[23] These TGA results suggest that the membranes are sufficiently thermally stable to be used under the operating conditions of fuel cells (80 °C).

3.3. Ion exchange capacity

Ion exchange capacity (IEC) is an important factor that influences the water uptake and swelling of membranes. The calculated and titrated IECs of the membranes are listed in Table 1. The titrated IEC of PAES-TA-OH was 1.31 meq/g, which is in good accordance with the calculated IEC (1.43 meq/g). However, the titrated IEC of cPAES-TA-OH was lower than the calculated value. There can be two reasons for this observation. First, the IEC of triazolium cations was poor compared with that of QA groups, which might be attributed to the strong binding energy between triazolium cations and counter anions.[24] Second, cPAES-TA-OH probably forms dense and compact network structures after crosslinking. Therefore, the triazolium cations may be under steric hindrance due to the hydrophobic hexane crosslinker and the PAES backbone, interrupting ion exchange.[12] Nevertheless, the IEC value of cPAES-TA-OH was higher than that of PAES-TA-OH because additional triazolium cations were formed during the crosslinking process. This is a huge advantage considering that crosslinking generally lowers the IEC.[25]

3.4. Water uptake and swelling ratio

The water uptake and swelling ratio significantly influence the hydroxide conductivity and dimensional stability of AEMs. Water uptake of PAES-TA-OH and cPAES-TA-OH was carefully measured at different temperatures (30 °C and 80 °C). As shown in Figure 5(a), the water uptake of PAES-TA-OH and cPAES-TA-OH was higher at 80 °C than that measured at 30 °C. This is probably attributed to the increased volume of micropores in the membranes at higher temperatures.[26] Both membranes exhibited moderate water uptake values for AEM applications. In particular, it should be noted that cPAES-TA-OH had a slightly higher water uptake than did PAES-TA-OH at both temperatures. Normally, membrane crosslinking leads to the formation of a compact network structure with less free volume, thus lowering the water uptake.[6,7,25] In the case of cPAES-TA-OH, however, higher IEC might lead to higher water uptake.

The swelling ratio of the membranes showed a similar tendency to that of water uptake (Figure 5(b)). The swelling ratios of PAES-TA-OH and cPAES-TA-OH were higher at 80 °C because their water uptake values were higher at 80 °C. Moreover, cPAES-TA-OH showed slightly higher swelling ratios of 3.9% and 9.1% at 30 °C and 80 °C, respectively, than those of PAES-TA-OH (3.1% and 8.3% at 30 °C and 80 °C, respectively) because of the higher water uptake of cPAES-TA-OH.

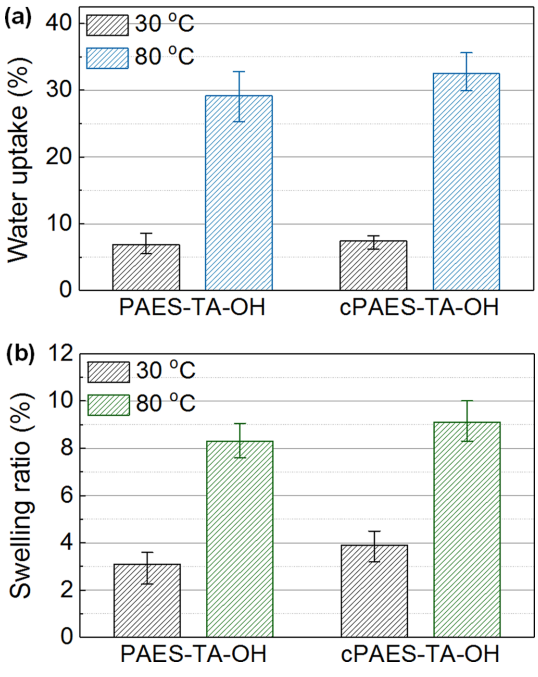

Figure 5. (a) Water uptake and (b) swelling ratios of PAES-TA-OH and cPAES-TA-OH at 30 °C and 80 °C.

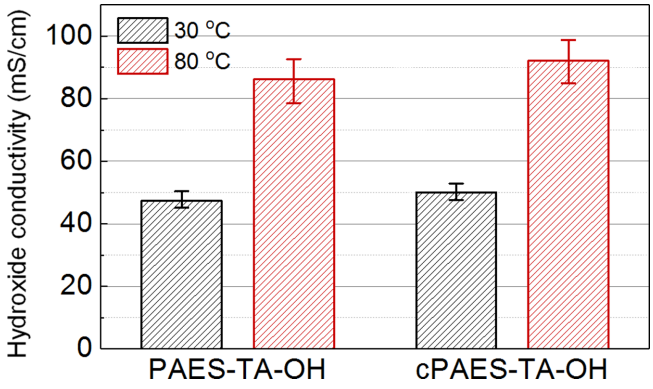

Figure 6. Hydroxide conductivity of PAES-TA-OH and cPAES-TA-OH at 30 °C and 80 °C under 95% RH.

3.5. Hydroxide conductivity and alkaline stability

For effective AEM applications, high anion conductivity is considered an essential factor to reduce the membrane resistance in membrane electrode assemblies.[1] Hydroxide conductivities of PAES-TA-OH and cPAES-TA-OH were also measured at 30 °C and 80 °C (Figure 6). Similar to the results of water uptake and swelling ratio, both membranes showed higher hydroxide conductivity at 80 °C (86.2 mS/cm and 92.1 mS/cm for PAES-TA-OH and cPAES-TA-OH, respectively), which are reasonable values for AEMFCs. In addition, higher hydroxide conductivity of cPAES-TA-OH than that of PAES-TA-OH was observed at 30 °C and 80 °C because of the higher water uptake of cPAES-TA-OH (normally, hydroxide conductivity is mainly influenced by water uptake). The hydroxide conductivities were superior or comparable compared with the state-of-the-art AEMs in spite of the lower or similar IEC of the membranes.[4,15,27]

Excellent alkaline stability of AEMs is one of the most desirable properties for long-term and high-performance fuel cell operation.[2] Most AEMs suffer from degradation under alkaline conditions including benzyl substitution, β-hydrogen elimination, direct nucleophilic substitution at α-carbon, and *N*-ylide formation.[3,28,29] The alkaline stabilities of PAES-TA-OH and cPAES-TA-OH were compared after immersing the membranes in 1 M NaOH at 80 °C for 24 h. The alkaline stability could be evaluated from the reduced ratio of hydroxide conductivity before and after the test. As shown in Figure 7, PAES-TA-OH and cPAES-TA-OH retained 51% and 67% of the initial hydroxide conductivity, respectively, after the stability test. These results indicate that the crosslinked structure of AEMs can be effective in reducing degradation in harsh alkaline environments since the compact network structure blocks the penetration of hydroxide anion into the membranes.[19]

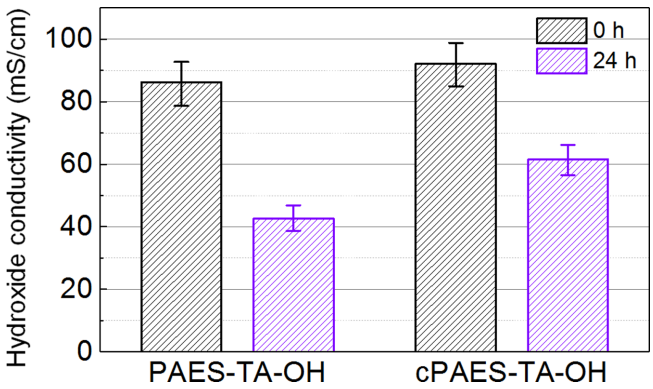

Figure 7. Hydroxide conductivities of PAES-TA-OH and cPAES-TA-OH at 80 °C under 95% RH after alkaline stability tests by immersing in 1 M NaOH at 80 °C for 24 h.

4. Conclusions

A crosslinked PAES AEM containing QA and triazolium cations (cPAES-TA-OH) was prepared by a click reaction, followed by *in-situ* casting and crosslinking in order to investigate the crosslinking effect on membrane performance. The increased number of cations (formation of triazolium cations) by crosslinking resulted in improved IEC, leading to higher water uptake, higher swelling, and higher hydroxide conductivity, as compared to those obtained using a non-crosslinked membrane (PAES-TA-OH). Crosslinking was also advantageous to alkaline stability because the compact and dense network structures of cPAES-TA-OH reduced the alkaline degradation. The formation of additional triazolium cations from the crosslinking led to the unexpected phenomenon and offset the trade-off between conductivity and stability of AEMs. Considering the enhanced hydroxide conductivity and membrane stability by a simple crosslinking strategy, cPAES-TA-OH could be a promising polymer electrolyte membrane for AEMFCs.

References

(1) J. Ran, L. Wu, Y. Ru, M. Hu, L. Din, and T. Xu, *Polym. Chem.*, **6**, 5809 (2015).
(2) P. Jannasch and E. A. Weiber, *Macromol. Chem. Phys.*, **217**, 1108 (2016).
(3) D. Yun, T. Yim, O. J. Kwon, and T.-H. Kim, *Macromol. Res.*, **27**, 1050 (2019).
(4) J. R. Varcoe and R. C. Slade, *Fuel Cells*, **5**, 187 (2005).
(5) J. Choi, J.-H. Jang, J. E. Chae, H.-Y. Park, S. Y. Lee, J. H. Jang, J. Y. Kim, D. Henkensmeier, S. J. Yoo, K. Y. Lee, Y.-E. Sung, and H.-J. Kim, *Macromol. Res.*, **28**, 275 (2020).
(6) W. Liu, L. Liu, J. Liao, L. Wang, and N. Li, *J. Membr. Sci.*, **536**, 133 (2017).
(7) K. H. Lee, D. H. Cho, Y. M. Kim, S. J. Moon, J. G. Seong, D. W. Shin, J.-Y. Sohn, J. F. Kim, and Y. M. Lee, *Energy Environ. Sci.*, **10**, 275 (2017).
(8) M. E. Tuckerman, D. Marx, and M. Parrinello, *Nature*, **417**, 925 (2002).
(9) S. Noh, J. Y. Jeon, S. Adhikari, Y. S. Kim, and C. Bae, *Acc. Chem. Res.*, **52**, 2745 (2019).
(10) Q. Ge, J. Ran, J. Miao, Z. Yang, and T. Xu, *ACS Appl. Mater. Interfaces*, **7**, 28545 (2015).
(11) N. Li, M. D. Guiver, and W. H. Binder, *ChemSusChem*, **6**, 1376 (2013).
(12) L. Liu, S. He, S. Zhang, M. Zhang, M. D. Guiver, and N. Li, *ACS Appl. Mater. Interfaces*, **8**, 4651 (2016).
(13) M.-K. Ahn, B. Lee, J. Jang, C.-M. Min, S.-B. Lee, C. Pak, and J.-S. Lee, *J. Membr. Sci.*, **560**, 58 (2018).
(14) L. Zeng and T. Zhao, *J. Power Sources*, **303**, 354 (2016).
(15) S.-B. Lee, C.-M. Min, J. Jang, and J.-S. Lee, *Polymer*, **192**, 122331 (2020).
(16) J. Han, L. Zhu, J. Pan, T. J. Zimudzi, Y. Wang, Y. Peng, M. A. Hickner, and L. Zhuang, *Macromolecules*, **50**, 3323 (2017).
(17) J. Jang, D.-H. Kim, M.-K. Ahn, C.-M. Min, S.-B. Lee, J. Byun, C. Pak, and J.-S. Lee, *J. Membr. Sci.*, **595**, 117508 (2020).
(18) H. Hu, T. Dong, Y. Sui, N. Li, M. Ueda, L. Wang, and X. Zhang, *J. Mater. Chem. A*, **6**, 3560 (2018).
(19) W. Ma, C. Zhao, J. Yang, J. Ni, S. Wang, N. Zhang, H. Lin, J. Wang, G. Zhang, Q. Li, and H. Na, *Energy Environ. Sci.*, **5**, 7617 (2012).

(20) N. Chen, C. Long, Y. Li, C. Lu, and H. Zhu, *ACS Appl. Mater. Interfaces*, **10**, 15720 (2018).
(21) J. Wang, G. He, X. Wu, X. Yan, Y. Zhang, Y. Wang, and L. Du, *J. Membr. Sci.*, **459**, 86 (2014).
(22) M. Teresa Pérez-Prior, N. Ureña, M. Tannenberg, C. del Río, and B. Levenfeld, *J. Polym. Sci., Part B: Polym. Phys.*, **55**, 1326 (2017).
(23) E. A. Weiber, D. Meis, and P. Jannasch, *Polym. Chem.*, **6**, 1986 (2015).
(24) F. Zapata, L. Gonzalez, A. Caballero, I. Alkorta, J. Elguero, and P. Molina, *Chem. Eur. J.*, **21**, 9797 (2015).
(25) L. Zhu, T. J. Zimudzi, N. Li, J. Pan, B. Lin, and M. Hickner, *Polym. Chem.*, **7**, 2464 (2016).
(26) Y. Li, T. Zhao, and W. Yang, *Int. J. Hydrogen Energy*, **35**, 5656 (2010).
(27) E. N. Hu, C. X. Lin, F. H. Liu, Q. Yang, L. Li, Q. G. Zhang, A. M. Zhu, and Q. L. Liu, *ACS Appl. Energy Mater.*, **1**, 3479 (2018).
(28) C. Macomber, J. Boncella, B. Pivovar, and J. Rau, *J. Therm. Anal. Calorim.*, **93**, 225 (2008).
(29) B. R. Einsla, S. Chempath, L. Pratt, J. Boncella, J. Rau, C. Macomber, and B. Pivovar, *ECS Trans.*, **11**, 1173 (2007).

